

HOMOGENIZATION OF METAMATERIAL-LOADED SUBSTRATES AND SUPERSTRATES FOR ANTENNAS

A. Semichaevsky and A. Akyurtlu

Department of Electrical and Computer Engineering
University of Massachusetts
1 University Avenue, Lowell, MA 01854, USA

Abstract—This article deals with an approach to the design of planar antennas that use metamaterial-loaded substrates based on the effective medium approximations. Metamaterials are structured composite materials with unique electromagnetic properties due to the interaction of electromagnetic waves with the finer scale periodicity of conventional materials. They may be used to modify the effective electromagnetic parameters of planar antenna substrates and to design antennas with the improved coupling to the feed, increased impedance matching bandwidths, miniaturized dimensions, and narrower beamwidths compared to those that use conventional dielectric materials for the same purposes. The electromagnetic analysis and optimization based on the effective medium approximations of metamaterials is very convenient since it deals with only a few bulk medium parameters instead of a large number of parameters describing a discrete structure. At the same time, the most common way of obtaining these effective medium parameters is transmission/reflection simulations or measurements in free space or in a homogeneous background medium. For a host medium which is not homogeneous, as for a grounded substrate, the effective medium parameters are different from the free space ones. The scattering losses in a metamaterial medium need to be accurately taken into account and included as parameters in full-wave bulk medium models. For this reason, in the effective medium approach for antenna substrates, one needs to use the appropriate effective medium approximations that take the coupling between inclusions into account and also to evaluate the effects of the scattering losses. In practice, this is done by finding the effective medium parameters inside an arbitrary substrate medium, and not in a homogeneous host medium or in free space. This paper presents the methodology and the results of FDTD analysis of planar antennas that have substrates

with various metamaterial inclusion densities. The effective bulk medium approach presented in the article is analyzed by comparing the antenna return losses and radiation patterns to the ones computed for a discrete structure. The Green's function of the host medium (antenna substrate) is used to calculate the approximate bulk effective medium parameters of the MTM-loaded substrate.

1. INTRODUCTION

Applications of metamaterials in antenna design have been considered in recent years by several authors [1–7]. The electromagnetic analysis of metamaterial-based antennas was carried out using full-wave modeling and multi-domain discretization of antenna substrate dielectric properties [5], transmission line analogies [1], and the lumped embedded circuit approach [7]. In [4], the substrate medium was already considered to be homogenized and the problem was solved analytically. Effective medium parameters of composite electromagnetic materials used in such antennas can be obtained through various homogenization methods [8–10]. The homogenization can substantially simplify the electromagnetic analysis since the electromagnetic wave interaction problem is thereby reduced to the analysis of the homogeneous bulk medium.

A reduction in the number of effective medium parameters associated with the metamaterial embedded in a planar antenna substrate makes the optimization of an antenna with respect to several parameters (the minimum return loss and the maximum impedance-matching bandwidth) simpler. The effective medium parameters of the substrate may be perturbed by various proximity coupling effects compared to the ones extracted from full-wave simulations for an infinite lattice. However, as it will be shown in this paper using numerical validations, these perturbations are often small and the loaded substrate can still be modeled as a bulk material.

This paper is concerned with the estimation of effective medium parameters for metamaterials embedded in an antenna substrate and their use in antenna analysis. Furthermore, the interactions between inclusions in a 2D periodic lattice embedded in an antenna substrate are calculated and effective propagation constants are found. Several examples of antenna designs are used to validate the homogenization procedures by comparing return losses and radiation patterns for substrates loaded with discrete structures and the ones that are described by the corresponding bulk effective medium model.

2. METHODOLOGY

2.1. Background

Some of the previously published papers dealing with the analysis and optimization of metamaterial-loaded antenna substrates [5] have considered full-wave analysis of MTM structures using the density method, with a fine discretization of the substrate into homogeneous domains. As it could be expected, this entailed a large number of parameters used in the optimization, while the optimal solutions were sensitive to the variations in antenna geometry and required a new global optimization to be carried out for any change in the boundary conditions or geometry. Analytical methods for metamaterial homogenization in the static (low-frequency) limit have been proposed by Silveirinha [11] and Tretyakov [12]. These methods allow obtaining effective medium parameters for composite materials consisting of infinitely-long PEC wires.

The electromagnetic response of a single unit MTM cell can also be approximated by an embedded equivalent circuit [7]. The expressions provided in [7] are suitable for calculating effective propagation constants in a MTM-loaded substrate, however, the scattering losses are not included in the formulas for the effective permeability explicitly, and the only losses considered were the Ohmic losses in the conductor material.

The homogenization of a metamaterial in a wide frequency range can be carried out by extracting its effective medium electric polarizability and magnetization of a single MTM inclusion [14, 15] from plane wave scattering experiments. Under this approach, each unit cell in an infinitely-periodic metamaterial lattice is characterized by its effective electric and magnetic polarizability tensors $\bar{\epsilon}$ and $\bar{\mu}$ and magneto-electric coupling tensors $\bar{\zeta}$ and $\bar{\xi}$. The electric and magnetic moments can be related to the total electric and magnetic fields using polarizability matrices as follows:

$$\begin{bmatrix} \vec{p} \\ \vec{m} \end{bmatrix} = [\bar{\alpha}] \begin{bmatrix} \vec{E}_t \\ \vec{H}_t \end{bmatrix}, \quad [\bar{\alpha}] = \begin{bmatrix} \bar{\alpha}_{ee} & \bar{\alpha}_{em} \\ \bar{\alpha}_{me} & \bar{\alpha}_{mm} \end{bmatrix} \quad (1)$$

where subscript t refers to the total field.

There exist some metamaterial structures such as the pairs of split ring resonators (SRR) with the opposing directions of the open wire loops [1], for which the contributions of magnetoelectric coupling ($\bar{\alpha}_{em}$ and $\bar{\alpha}_{me}$) can be neglected.

Full-wave FDTD calculations allow obtaining currents flowing in the inclusions directly, and the subsequent volume integration can be

used to calculate the polarization/magnetization responses. Thus, when there is no magnetoelectric coupling assumed, the effective medium parameters are:

$$\begin{aligned}\bar{\epsilon} &= \epsilon_0 (\bar{\epsilon}_r + \bar{\alpha}_{ee}N) \\ \bar{\mu} &= \mu_0 (\bar{\mu}_r + \bar{\alpha}_{mm}N)\end{aligned}\quad (2)$$

where $\bar{\epsilon}_r$ and $\bar{\mu}_r$ are the relative permittivity and permeability of the homogeneous background medium, N is the volumetric density of inclusions. The effective permeability and permittivity of the inclusions embedded in a substrate that has its Green's function different from the one of the homogeneous medium require a different approach to their analysis. The following section describes our approach to the analysis of MTM-loaded substrates for antenna applications.

2.2. Analysis of the Embedded Metamaterial Effective Properties

Figure 1 illustrates the geometry of the problem solved in this section. An infinite PEC-backed dielectric slab is loaded with magnetic SRR inclusions with polarizability matrices known from previous calculations, and the dominant incident plane wave component is described by wavevector \vec{k} and vector fields \vec{E} and \vec{H} . The values of the effective medium permittivity and permeability for use in a bulk dispersive model of the substrate need to be found. In addition, some conducting antenna topology may be printed on the substrate surface.

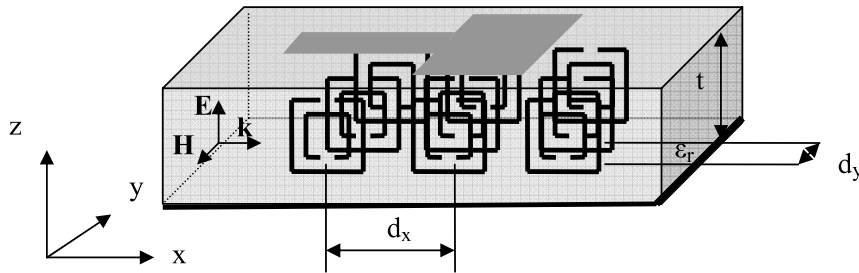


Figure 1. Electromagnetic wave interaction with magnetic metamaterial embedded in grounded slab that is used as an antenna substrate.

In the analysis of effective medium parameters (homogenization), electric, magnetic and magneto-electric polarizability matrices $\bar{\alpha}_{ee}, \bar{\alpha}_{mm}, \bar{\alpha}_{em}, \bar{\alpha}_{me}$ are found for a single isolated inclusion. The

host medium Green's function is used to obtain the effective polarizability matrices for the semi-infinite lattice inside the substrate: $\overline{\alpha}'_{ee}, \overline{\alpha}'_{mm}, \overline{\alpha}'_{em}, \overline{\alpha}'_{me}$.

The quasistatic approximation for the interaction matrix [15] is not suitable for solving this problem because the Green's function of the host medium may be any, and the equations obtained for free space cannot be applied to the case of the arbitrary host medium. Let us assume that the linear field response tensor [16] is found from either analytical formulas or numerical calculations. As in other homogenization methods, inclusions with diameter D are assumed to be small compared to the wavelength in the medium ($D < \lambda/4$). Then for the two interacting scatterers inside the host medium, the interactions can be found from the scattering theory. Since the effective polarizabilities of inclusions and the medium response are known, the vectorial scattering equation [16] can be written applying the multiple scattering formalism in a way similar to the one provided in [17, p. 709]. Since the polarizabilities in our model are associated with a point scatterer, using the sampling property of the spatial δ -function, this equation can be written as follows:

$$\begin{aligned} \begin{bmatrix} \vec{E}_t(\vec{r}) \\ \vec{H}_t(\vec{r}) \end{bmatrix} &= \begin{bmatrix} \vec{E}(\vec{r}) \\ \vec{H}(\vec{r}) \end{bmatrix} + \int_V \overline{\overline{G}}(\vec{r}, \vec{r}') N \overline{\alpha}(\vec{r}') \begin{bmatrix} \vec{E}(\vec{r}') \\ \vec{H}(\vec{r}') \end{bmatrix} d^3\vec{r}' \\ &+ \iint_V \overline{\overline{G}}(\vec{r}, \vec{r}') N \overline{\alpha}(\vec{r}') \overline{\overline{G}}(\vec{r}', \vec{r}'') N \overline{\alpha}(\vec{r}'') \begin{bmatrix} \vec{E}(\vec{r}') \\ \vec{H}(\vec{r}') \end{bmatrix} d^3\vec{r}' d^3\vec{r}'' \\ &+ \dots = \begin{bmatrix} \vec{E}(\vec{r}) \\ \vec{H}(\vec{r}) \end{bmatrix} + \overline{\overline{G}}(\vec{r}, \vec{r}') N \overline{\alpha}(\vec{r}') \begin{bmatrix} \vec{E}(\vec{r}') \\ \vec{H}(\vec{r}') \end{bmatrix} \\ &+ \overline{\overline{G}}(\vec{r}, \vec{r}') N \overline{\alpha}(\vec{r}') \overline{\overline{G}}(\vec{r}', \vec{r}') N \overline{\alpha}(\vec{r}') \begin{bmatrix} \vec{E}(\vec{r}') \\ \vec{H}(\vec{r}') \end{bmatrix} + \dots \quad (3) \end{aligned}$$

where \vec{r}' and \vec{r}'' are the coordinates of the first and the second point scatterer and the integrals over the volume of the unit cell V are three-fold. When the higher order terms ($n > 1$) in (3) are much smaller than the single scattering term and can be neglected,

$$\begin{bmatrix} \vec{E}_t \\ \vec{H}_t \end{bmatrix} \approx \begin{bmatrix} \vec{E} \\ \vec{H} \end{bmatrix} + \overline{\overline{G}} N \overline{\alpha} \begin{bmatrix} \vec{E} \\ \vec{H} \end{bmatrix} = \{ \overline{\overline{I}} + \overline{\overline{G}} N \overline{\alpha} \} \begin{bmatrix} \vec{E} \\ \vec{H} \end{bmatrix} \quad (4)$$

Thus, if the magnitudes of the spatial response tensor components $\overline{\overline{G}}(\vec{r}, \vec{r}')$ decay rapidly enough with distance, then two assumptions can be made, namely that only the nearest neighboring inclusions

interact and that the interactions are predominantly single scattering. These assumptions will not be applicable when the volumetric density of inclusions is high.

By comparing equations (1) and (4), it can be seen that under the single scattering approximation and assuming that the MTM inclusions can be represented by point scatterers polarizability $\bar{\alpha}$, the effective polarizability of a single lattice cell of a periodic inclusion lattice can be found as:

$$\bar{\alpha}' = \bar{\alpha} \left[\bar{I} + \sum_i^{N_n} \bar{G}_i N \bar{\alpha} \right] \quad (5)$$

where index i refers to the summation of scattered field contributions by other inclusions, N_n is the number of the nearest neighbors of an inclusion.

If the host medium is homogeneous, then in the limit of single scattering of inclusions and for small argument $\bar{G}(\vec{r}, \vec{r}') N \bar{\alpha}$, the homogenization procedure in this paper is equivalent to the quasistatic homogenization approach [15]: the linear response $\bar{G}(\vec{r}, \vec{r}')$ can be replaced with the quasistatic interaction constant \bar{C} , and $[\bar{I} - \bar{C} N \bar{\alpha}]^{-1} \approx [\bar{I} + \bar{G} N \bar{\alpha}]$.

It is worth mentioning that our homogenization procedure is derived for one incident wavevector, for instance, for a quasi-TEM wave introduced in the patch antenna via a microstrip line feed. An expansion to multiple incident wavevectors is straightforward. The perturbations due to the finite substrate or the interaction with the printed antenna topology are also not taken into account.

In summary, our homogenization procedure includes the following steps:

- 1) Find the polarizability tensor of a single inclusion;
- 2) Assume some volumetric density of inclusions in a periodic lattice, N ;
- 3) Find the frequency-dependent anisotropic spatial linear response tensor of the substrate to the embedded electric and magnetic dipoles;
- 4) Apply an approximation of the multiple scattering equation (3) and find the effective polarizability of a periodic lattice of inclusions in a substrate;
- 5) Find the effective permittivity and permeability of the periodic lattice, in accordance with equation (2);

The practical aspects of calculating the response of the embedded MTM lattice to the incident field will be considered in Subsection 2.4 of this paper.

This approach to modeling the wave propagation in loaded substrates is versatile and applicable to any metamaterial inclusions since it allows one to take into account the medium anisotropy and chirality and to use them in the bulk dispersive models of the substrate media. In all numerical validations in this paper, for the sake of simplicity, an assumption is made that the effective medium parameters contain no magnetoelectric coupling terms.

As it will be shown in the next subsection, the high density of inclusions allows obtaining higher real part of effective permeability near the resonance which is beneficial to the miniaturization of antenna designs. However, then the design of an actual antenna structure may be complicated since the interaction constants cannot be obtained in a closed form.

A general analysis of the embedded metamaterial was presented in this subsection. The following two sections deal with the analysis of effective medium parameters, and the numerical spatial response tensor calculations, as detailed in this section, for a substrate. First the effective bulk material refractive indices for inclusions in an unbounded homogeneous medium are found for different inclusion densities, then the scattering losses of a semi-infinite MTM structure are calculated for the PEC SRR medium in terms of the radiation resistances and compared to the previously published analytical results for open loop resonators of the same radius at the same signal frequency.

2.3. Effective Medium Parameters and Scattering Losses in Metamaterial

One of the obvious advantages of the homogenization approach described above is that it allows taking the scattering losses of inclusions into account directly, while this is more complicated when other homogenization methods, such as the lumped element method [1,7], are used. The following analysis deals with the scattering loss effects for a semi-infinite lattice of split-ring resonators in a homogeneous host medium.

It has been previously shown that the effective permeability tensor of an infinite array of split ring resonators is close to uniaxial [15,18]. According to our estimations, one of the tensor elements of the permeability tensor can be reasonably approximated by a second

order rational function, as follows:

$$\mu_{ii} = \mu_0 \left(\frac{a_2\omega^2 + a_1\omega + a_0}{\omega_0^2 - \omega^2 - j2\delta_h\omega_0\omega} \right), \quad \mu_{jj} = \mu_{kk} = \mu_0 \quad (6)$$

where i,j,k correspond to either x,y , or z in the order determined by the spatial orientation of the inclusion, ω_0 is the resonant frequency and δ_h is the damping factor. The accuracy of the second-order rational function fitting will be assessed in Appendix A of this paper.

For a MTM structure, the value of effective permittivity in (6) depends on the density of inclusions, according to (4), and is affected by the multiple scattering that is a function of the distance between them, according to (3).

Developing the previous section arguments, as an example of the cumulative effects of the density and electromagnetic interactions between inclusions on the effective refractive index were calculated for a lattice of SRRs with the outer ring diameter $D = 3.6$ mm in free space for different spacings d_y (referring to Figure 1). The analysis was done with FDTD and the parameter extraction was carried out according to [19]. Figure 2a illustrates the effects of the real part of the real refractive index and Figure 2b, the same effects but on the imaginary part of effective refractive index.

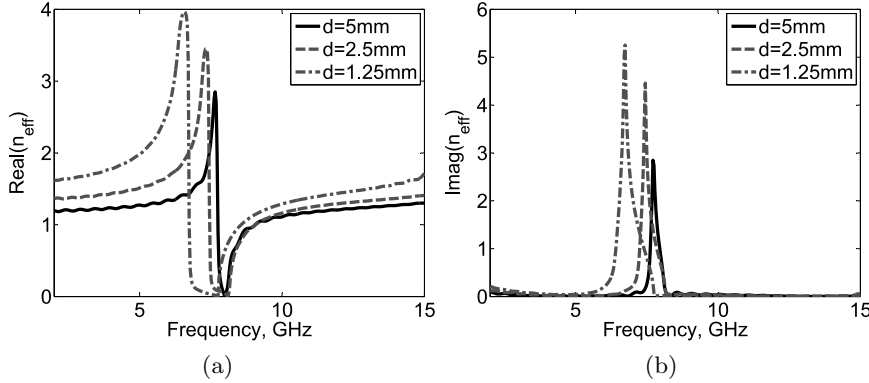


Figure 2. Effective refractive index of a semi-infinite SRR lattice in free space as a function of frequency for different inclusion spacings, (a) real part, (b) imaginary part.

The conclusions that can be drawn from simulation results shown in Figures 2a and 2b are that the decrease in inclusion spacing results in higher peak values of the real part of the effective refractive index and lower resonant frequency. At the same time, the half-width of

the resonance increases. The first effect is consistent with (4), while the latter two can only be explained by the effects of mutual coupling between inclusions in the SRR lattice.

One of the parameters in (6) is the damping factor; its analysis is the subject of the following discussion. The resonant frequency of an isolated SRR can be found as:

$$\omega_0 = \frac{1}{\sqrt{LC}} \quad (7)$$

where L and C are the open loop inductance and the gap capacitance, respectively. At the same time, the wire loop inductance [20] can be calculated as:

$$L = \mu_0 b \left(\log \left(\frac{8b}{a} \right) - 2 \right), \quad (8)$$

where a is the radius of the wire, b is the radius of the circular loop, μ_0 is the permeability of free space.

The damping factor in (6) can also be expressed in terms of the radiation resistances of inclusions. The radiation resistance of a structure can be defined as:

$$R_r = \frac{2P_r}{|I|^2} \quad (9)$$

where P_r is the radiated power, I is the current flowing from the feed into the structure. In this context, metamaterial inclusions can be treated as wire loop antennas that reradiate some part of the incident electromagnetic wave. It is well known that the radiation resistance of an open wire loop is proportional to $(\frac{D}{\lambda})^2$, where D is the diameter of the inclusion and λ is the wavelength in the medium in which the inclusion is embedded. Thus, the reduction in the effective loss can be achieved by using the space-filling curves [22, 23].

FDTD simulations with periodic boundary conditions are run and effective permeability of the medium is found. The obtained complex μ_{eff} is then fitted with a second order rational function (6), and the damping factor δ is estimated. It is then assumed that the relationship between the quality factor Q and the other parameters of the Lorentzian resonator is [24]:

$$\omega_0(R_\Omega + R_r)C_g = 1/Q = \frac{2\delta^2\omega_0^2}{\sqrt{\omega_0^2 - 2\delta^2\omega_0^2}} \quad (10)$$

The gap capacitance of an open loop resonator is found from the resonance condition (10): $C_g = \frac{1}{\omega_0^2 L}$. Assuming that the Ohmic

resistance of the inclusion material $R_\Omega = 0$,

$$R_r = \frac{2\delta^2\omega_0^2}{\sqrt{\omega_0^2 - 2\delta^2\omega_0^2}}L\omega_0 \quad (11)$$

Let us assume that inductance of the loop L can be calculated from (8), and take into consideration that the resonant frequency for a double SRR with the outer ring radius of 1.2 mm and wire radius of 0.12 mm is 11.5 GHz in free space. The damping factor of the SRR was estimated by fitting the extracted effective permeability to be $\delta = 0.0157$. For an open square wire loop with the same radii of the loop and wire, this resonant frequency is 13.5 GHz in free space, and the damping factor is $\delta = 0.0133$. Radiation resistances for these types of MTM inclusions were calculated using (11) from numerical simulations and also found in literature for the same ratio of the loop and wire diameters, and the comparison of the results is presented in Table 1.

Table 1. Comparisons between the radiation resistance values at resonance for various inclusions.

Inclusion type	Radiation resistance, Ω	Source
SRR in a cubic lattice	7.43	This paper
Wire loop in a cubic lattice	7.48	This paper
Open wire loop	4.54	[27]

As one can see from Table 1, the split ring resonators in a cubic lattice have the same order of magnitude but higher radiation resistances than a single circular open wire loop. The detailed analysis of the differences between these results is left out of the scope of this paper, however, it is worth mentioning that among the reasons there may be the effects of the resonator shape and the effects of the lattice.

Once the electromagnetic response of an isolated inclusion is known, the Green's function of the host medium needs to be found and the effective medium parameters of the loaded substrate medium need to be obtained.

2.4. Analysis of the Green's Function of the Substrate

The electromagnetic interaction problem for a known response of a single inclusion can be solved if the Green's function of the host

medium is known. The methodology for calculating the bulk effective medium parameters for a semi-infinite lattice of embedded MTM inclusions was outlined in Subsection 2.2 of this paper.

In some cases, the Green's function can be found analytically. An analysis of the wave propagation in grounded slabs with metamaterials can also be found in [25]. The host medium Green's function (medium spatial linear response tensor to electric and magnetic sources) computed numerically using FDTD and the impressed electric and magnetic dipole sources. The electric field E_z component is excited at a single FDTD cell, representing a vertical electric dipole, and all field components are recorded at various distances from the source. Similarly, E_y component is excited at a single cell that corresponds to the horizontal electric dipole location and all field components are recorded at various distances from the source. By analogy, Green's function elements for the H -field are found.

The magnitudes of the electrical and magnetic Green's functions of the substrate as functions of distance from the source at 7.75 GHz signal frequency, for the source located at the depth of 1.25 mm in a 2.5 mm-thick grounded substrate with permittivity $\epsilon_r = 2.2$, are shown in Figure 3.

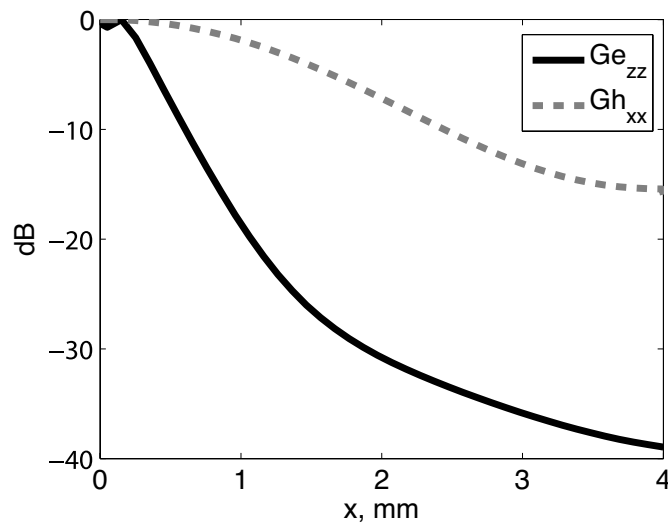


Figure 3. Electric and magnetic components of the Green's function of the dielectric substrate evaluated at different distances from the source at 7.75 GHz frequency, the sources are located at the depth of 1.25 mm in a 2.5 mm-thick grounded substrate with permittivity $\epsilon_r = 2.2$.

As it can be seen from Figure 3, the magnitudes of the electric and magnetic responses suggest that the coupling between the inclusions due to magnetic interactions is substantially stronger than the one due to the electric interactions. The magnitudes of the magnetic components of the response tensor also suggest that multiple scattering by the inclusions can be strong when the inclusions are closely packed.

The polarizability tensor of a single inclusion $\bar{\alpha}$ in numerical examples will be assumed as uniaxial. This restriction is imposed because the Weir's extraction method is used to calculate the polarizabilities. In addition, an approximation that the scattering between adjacent inclusions was single, corresponding to a just one term in the series in equation (4), resulting in the effective medium tensor given by equation (5). The polarizability of an inclusion is calculated using the Weir's method with PEC and PMC boundary conditions for a plane incident wave propagating along one direction for a large spacing between inclusions so that the inclusions can be considered almost non-interacting. The μ_{yy} component is then extracted from the reflection and transmission coefficients, while μ_{xx} and μ_{zz} are assumed to be close to one. The electric response is found to be considerably smaller than the magnetic one and is ignored in the numerical simulations in Section 3. Then equation (5) is used to correct the effective polarizability of the embedded metamaterial for the effects of electromagnetic interactions, obtaining the effective polarizability matrix of a periodic lattice $\bar{\alpha}'$. These calculations are carried out for different signal frequencies.

It should be noted that two interrelated factors may be responsible for the effective polarizability of the MTM lattice embedded in the substrate: the electric and magnetic coupling that can be calculated using the interaction constants, and the density of inclusions that determines the magnitude of the electric and magnetic resonances. The effective medium model presented in this Section will be validated in Section 3.

3. NUMERICAL VALIDATION OF BULK DISPERSIVE SUBSTRATE MODELS

Numerical simulations included in this section will be used to analyze the FDTD bulk dispersive medium models for homogenized antenna substrates by comparing the characteristics of these antennas to the ones computed with FDTD for antennas loaded with discrete metamaterial structures. Figure 4 compares the return losses for patch antennas on MTM-loaded substrates computed with FDTD. One of these return losses is computed for an antenna on a substrate

loaded with periodic discrete SRR inclusions (label ‘Discrete SRR’), another return loss is computed using a bulk dispersive model for the effective medium permeability of the composite medium obtained from equations (2), (5) (label ‘Bulk medium, loaded substrate’), and the last one is for the effective permeability computed numerically for a homogeneous dielectric with $\epsilon_r = 2.2$ (label ‘Bulk medium, homogeneous dielectric’). The patch antenna has dimensions of 12.54×16 mm, is fed by a 50 Ohm line feed, and the thickness of the substrate is 5 mm. The embedded double split rings have the outer diameter of 4.8 mm, the gap of 0.48 mm and are arranged inside the substrate as shown in Figure 1 with the spacings $d_x = 5$ mm, $d_y = 5$ mm. The bulk model was obtained from the extracted effective medium parameters as discussed in Subsections 2.1 and 2.2 with a single scattering approximation (4) and implemented via the PLRC dispersive formulation of FDTD [26].

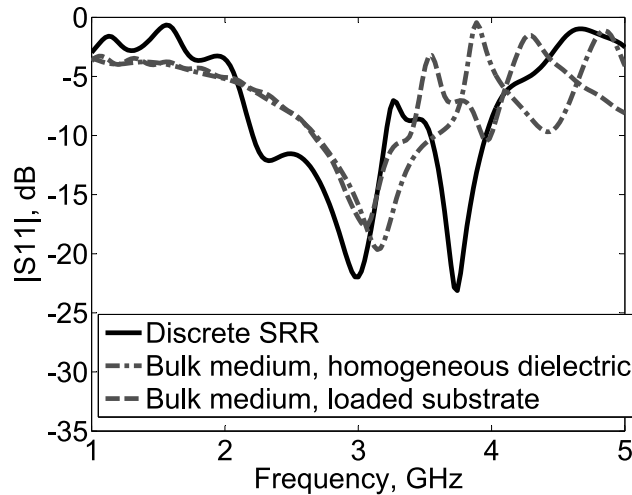


Figure 4. Return loss dependences for patch antennas on an SRR-loaded substrate ($D = 4.8$ mm) with inclusion spacing along y -axis of 5 mm, calculated with FDTD for a discrete metamaterial model and for a bulk effective medium model.

Results shown in Figure 4 indicate that the return losses of a MTM-loaded patch antenna calculated with the bulk embedded MTM model and the discrete MTM are close. The first two resonant frequencies are only different by several percent, and the magnitudes of the return losses at resonances are also comparable. At the same time, the return loss dependence computed using a bulk effective medium

for a homogeneous dielectric with embedded MTM inclusions of the same dimensions is less similar to the one for the discrete MTM case. The differences in the effective medium permeabilities computed with the two bulk models are in the resonant frequencies and the damping factors. When the effective permeability of the substrate is calculated, even in the single scattering approximation, using the spatial response tensor of the grounded slab, this produces a return loss dependence that is closer to the one for the discrete embedded MTM than the one for the effective permeability found using the full-wave calculation of the coupling but for the homogeneous host medium.

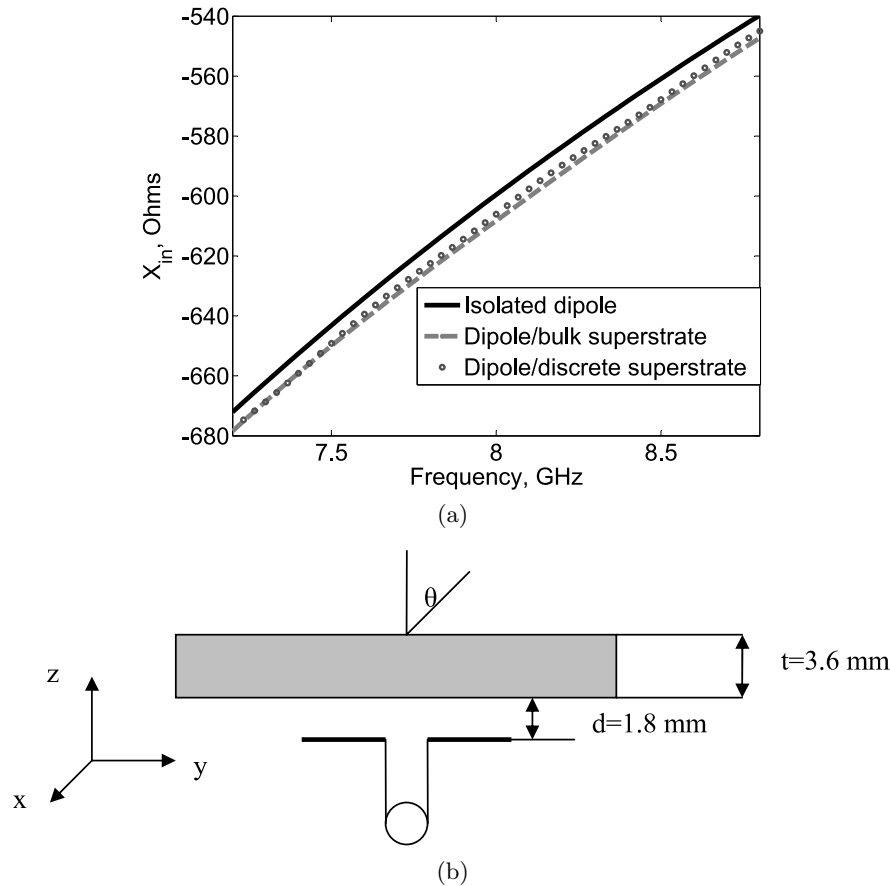


Figure 5. Comparison between the input reactances of a horizontal dipole in free space without superstrate, with discrete MTM superstrate and with a bulk MTM superstrate, a) input reactances, b) dipole-superstrate geometry.

In the second numerical simulation, the effects of the proximity coupling between an MTM-loaded superstrate and a dipole in free space on the dipole input impedance. A bulk dispersive anisotropic FDTD model for a discrete superstrate, a “homogenized” superstrate was calculated. The homogenization takes into account the full-wave interactions between inclusions using periodic boundary conditions and [19], since the structure resides in free space.

Figure 5a provides comparisons between the input reactances of a horizontal dipole of length $l = 3.6$ mm, wire radius $a = 0.07$ mm in free space in presence of an anisotropic superstrate (for its bulk and discrete representations) and without it. The superstrate has thickness of 3.6 mm and is placed 1.8 mm from the dipole. The discrete structure consists of double split rings. The split rings lie in the z - y plane, where dipole is along y -axis, and the discrete lattice has dimensions 8×4 resonators in the x - y plane. In the bulk model, the superstrate is considered to be uniaxial with μ_{yy} component assigned the dispersion while other components of $\bar{\mu}$ are assumed to be equal to one. Figure 5b shows the dipole-superstrate geometry used in this numerical experiment.

As the results shown in Figure 5 suggest, the effective bulk medium model and the discrete model for the MTM superstrate provide the reasonably close input reactances of the dipole antenna. At the same time, the frequency-dependent reactance of the dipole in free space is different from the ones computed for the dipole-superstrate structure. This suggests that the homogenization model is highly accurate.

4. CONCLUSIONS

Metamaterial-loaded planar antennas can be analyzed with sufficient accuracy assuming that a discrete metamaterial embedded in a substrate can be represented by an effective bulk model for electromagnetic parameters. Due to the reduced number of design parameters in the effective medium model as compared to the other substrate medium models, the analysis and optimization of the antenna can be substantially simplified.

The interactions between embedded inclusions can be properly taken into account if the polarizability and magnetization responses for a single isolated inclusion are known from either simulations or measurements. The anisotropic Green’s function and multiple scattering approaches allow computing the effective medium parameters that account for the coupling between inclusions inside an arbitrary substrate.

The analysis of electromagnetic interactions between MTM

inclusions in a host medium or in free space suggests that two phenomena can affect the effective medium parameters: the density of inclusions and the strength of mutual coupling that depends on the Green's function of the host medium and the distance between inclusions, i.e., on inclusion density. Thus, any effective medium model should take these effects into account.

Numerical calculations that were used to compare the models for the bulk and discrete embedded metamaterial showed that the frequency-dependent return losses of patch antennas calculated for the discrete structure and for the bulk medium agree reasonably. The input impedances for a dipole in presence of a dispersive anisotropic superstrate modeled using the bulk and discrete models are also close.

A certain advantage of the proposed homogenization approach is that it allows one to take into account the scattering/radiation losses in addition to the Ohmic losses in the inclusions. This is important when the MTM-loaded antenna characteristics are to be calculated with high accuracy.

APPENDIX A. SECOND ORDER RATIONAL FUNCTION FOR PERMEABILITY TENSOR COMPONENTS

This Appendix includes the validation of the equation (6) approximation for the effective medium permeability of a semi-infinite array of SRR inclusions.

Figures A1a and A1b present the real and imaginary parts of the effective refractive index for the incident wavevector perpendicular to the SRR slab, respectively. These were calculated by fitting the effective permeability of the SRR inclusion array with the second order rational function of frequency. The double split rings have outer diameters of 3.6 mm and are arranged in a cubic lattice with the lattice constant of 5 mm. The effective medium parameters were obtained for a semi-infinite lattice of SRRs in free space using transmission/reflection method [19] and periodic boundary conditions in FDTD.

The following bulk effective model parameters for the SRR lattice were obtained by polynomial fitting of the effective permeability of the medium, in reference to equation (10): $\omega_0 = 4.6585e10$ rad/s, $\delta_h = 0.004$, $a_2 = -1.2832 - j0.1052$, $a_1 = 2.3149e10 + j5.6731e9$, $a_0 = 1.8754e21 - j5.2666e19$.

An FDTD-PLRC model for equation (6) with these parameters is readily available.

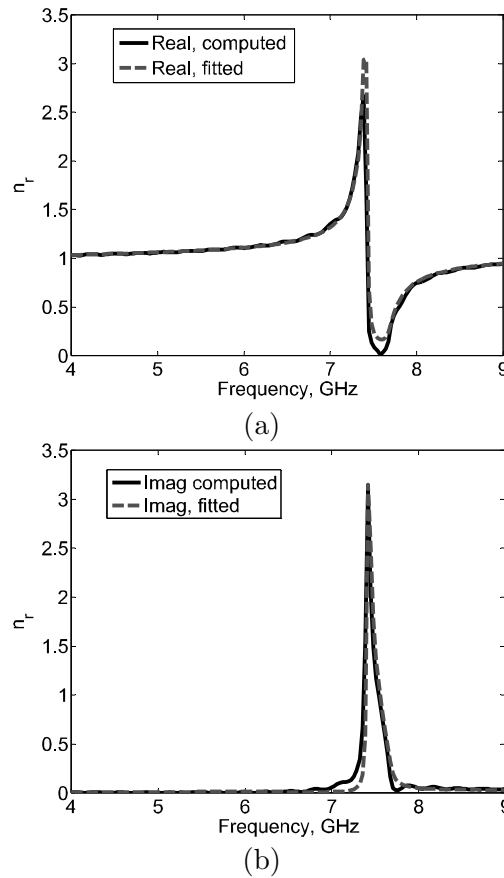


Figure A1. Refractive indices obtained as a result of fitting the effective permeability of an SRR with a second order rational function, (a) real part, (b) imaginary part.

REFERENCES

1. Ikonen, P., M. Karkkainen, and S. Tretyakov, "Experimental study of a $\lambda/2$ -patch antenna loaded with an array of metasolenoids as artificial magnetic substrate," *IEEE Antennas and Propagation Society International Symposium*, Vol. 2A, 606–609, July 3–8, 2005.
2. Ikonen, P., S. Maslovski, and S. Tretyakov, "PIFA loaded with artificial magnetic material: Practical example for two utilization strategies," *Microwave and Optical Technology Letters*, Vol. 46, No. 3, 205–210, 5 August 2005.

3. Wu, B.-I., W. Wang, J. Pacheco, X. Chen, T. Grzegorzcyk, and J. A. Kong, "A study of using metamaterials as antenna substrate to enhance gain," *Progress In Electromagnetics Research*, PIER 51, 295–328, 2005.
4. Xu, W., L. W. Li, H. Y. Yao, T. S. Yeo, and Q. Wu, "Left-handed material effects on waves modes and resonant frequencies: filled waveguide structures and substrate-loaded patch antennas," *Journal of Electromagnetic Waves and Applications*, Vol. 19, No. 15, 2033–2047, 2005.
5. Kiziltas, G., Y. Koh, J. L. Volakis, N. Kikuchi, and J. Halloran, "Optimum design and fabrication of volumetric graded substrate for a broad band miniature antenna," *IEEE Antennas and Propagation Society International Symposium*, Vol. 1, 485–488, 2003.
6. Lee, Y., H. Yang, and C. Parini, "Applications of Electromagnetic Bandgap (EBG) structures for novel communication antenna designs," *36th European Microwave Conference*, 1056–1059, Sept. 2006.
7. Mosallaei, H. and K. Sarabandi, "Design and modeling of patch antenna printed on magneto-dielectric embedded-circuit metasubstrate," *IEEE Trans. on Antennas and Propagat.*, Vol. 55, No. 1, 45–52, Jan. 2007.
8. Xu, W., L. W. Li, H. Y. Yao, T. S. Yeo, and Q. Wu, "Extraction of constitutive relation tensor parameters of SRR Structures using transmission line theory," *Journal of Electromagnetic Waves and Applications*, Vol. 20, No. 1, 13–25, 2006.
9. Weiglhofer, W. and A. Lakhtakia, *Introduction to Complex Mediums for Optics and Electromagnetics*, SPIE Press, 2003.
10. Caloz, B., A. Lai, and T. Itoh, "The challenge of homogenization in metamaterials," *New Journal of Physics*, Vol. 7, 1–15, 2005.
11. Silveirinha, M. G., "Additional boundary condition for the wire medium," *IEEE Trans on Antennas and Propagat.*, Vol. 54, No. 6, 1766–1780, June 2006.
12. Simovski, C. R., I. Kolmakov, and S. A. Tretyakov, "Approaches to the homogenization of periodical metamaterials," *International Conference on Mathematical Methods in Electromagnetic Theory*, 41–44, June 26–29, 2006.
13. Smith, D. R., W. J. Padilla, D. C. Vier, S. C. Nemat-Nasser, and S. Schultz, "Composite medium with simultaneously negative permeability and permittivity," *Phys. Rev. Lett.*, Vol. 84, 4184–4188, 2000.

14. Saadoun, M. M. and N. Engheta, "The pseudochiral Ω -medium: what is it? And what can it be used for?" *IEEE Antennas and Propagation Society International Symposium*, Vol. 4, 2038–2041, July 18–25, 1992.
15. Ishimaru, A., S.-W. Lee, Y. Kuga, and V. Jandhyala, "Generalized constitutive relations for metamaterials based on the quasi-static Lorentz theory," *IEEE Trans. on Antennas and Propagat.*, Vol. 51, No. 10, Part 1, 2550–2557, 2003.
16. Jackson, D., *Classical Electrodynamics*, 2nd edition, John Wiley and Sons, Inc., 1975.
17. Born, M. and E. Wolf, *Principles of Optics*, 7th edition, Cambridge University Press, 1999.
18. Marques, R., F. Mesa, J. Martel, and F. Medina, "Comparative analysis of edge- and broadside-coupled split ring resonators for metamaterial design — theory and experiments," *IEEE Trans. on Antennas and Propagat.*, Vol. 51, No. 10, Part 1, 2572–2581, 2003.
19. Weir, W. B., "Automatic measurement of complex dielectric constant and permeability at microwave frequencies," *Proceedings of the IEEE*, Vol. 62, 33–36, 1974.
20. Balanis, C., *Antenna Theory, Analysis and Design*, Harper and Row, New York, 1983.
21. Pendry, J. B., "Magnetism from conductors and other nonlinear phenomena," *IEEE Trans. on Microwave Theory and Tech.*, Vol. 47, No. 11, 2075–2084, 1999.
22. Best, S. R., "A Comparison of the resonant properties of small space-filling fractal antennas," *IEEE Antennas and Wireless Propagat. Lett.*, Vol. 2, 197–200, 2003.
23. Best, S. R., "A discussion on the properties of electrically small self-resonant wire antennas," *IEEE Antennas and Propagation Magazine*, Vol. 46, No. 6, 9–22, 2004.
24. Pozar, D., *Microwave Engineering*, 3rd edition, Wiley, 2004.
25. Li, C., Q. Sui, and F. Li, "Complex guided wave solutions of grounded dielectric slab made of metamaterials," *Progress In Electromagnetics Research*, PIER 51, 187–195, 2005.
26. Kelley, D. and R. Luebbers, "Piecewise linear recursive convolution for dispersive media using FDTD," *IEEE Trans. on Antennas and Propagat.*, Vol. 44, No. 6, 792–798, 1996.
27. Schrank, H. and J. D. Mahony, "Approximations to the radiation resistance and directivity of circular-loop antennas," *IEEE Antennas and Propagation Magazine*, Vol. 36, No. 4, 52–55, 1994.